# Stability of twisted states in power-law-coupled Kuramoto oscillators on a circle with and without time delay

Hae Seong Lee [1], Beom Jun Kim,[1,*] and Hye Jin Park [2,†]
[1]*Department of Physics, Sungkyunkwan University, Suwon 16419, Republic of Korea*
[2]*Department of Physics, Inha University, Incheon 22212, Republic of Korea*

(Received 17 January 2024; accepted 9 May 2024; published 4 June 2024)

Other than the fully synchronized state, a twisted state can also be an equilibrium solution in the Kuramoto model and its variations. In the present work, we explore the stability of the twisted state in Kuramoto oscillators put on a rim of a planar circle in the two-dimensional space in the presence of power-law decaying interaction strength ($\sim r^{-\alpha}$ with the distance $r$) and time delays due to a finite speed of information transfer. For example, our model can phenomenologically mimic a large sports stadium where many people try to sing or clap their hands in unison; the sound intensity decays with the distance and there can exist a time delay proportional to the distance due to the finiteness of sound speed. We first consider the case without the time delay effect and numerically find that stable twisted states emerge when the exponent $\alpha$ exceeds a critical value of $\alpha_c \approx 2$. In other words, for $\alpha < \alpha_c$, the fully synchronized state, not the twisted state, is the only stable fixed point of the dynamics. In our analytic approach, we also derive an equation for $\alpha_c$ and discuss its solutions. In the presence of time delay, we find that it is possible that the synchronized state becomes unstable while twisted states are stable.

DOI: 10.1103/PhysRevE.109.064203

## I. INTRODUCTION

Synchronization is an emergent phenomenon that can be easily found in our daily lives. Hand clapping [1–3], heartbeat [4], and walking of pedestrians [5,6] are popular examples showing synchronous behaviors. Interaction between agents is the key to synchronizing their phases, and the Kuramoto model [7,8] has nicely provided the conditions and properties of such synchronization [7–11].

It is well known that when interaction strength is large enough, phases of all oscillators become synchronized for fully connected oscillators. However, the synchronized state is not the only stationary solution in the Kuramoto-type models. Even in identical oscillators that have the same inherent frequency, a different type of stable state other than a fully synchronized one can appear depending on interaction patterns and initial conditions. One such state is a twisted state [12,13], characterized by consistent phase differences between consecutive oscillators. When both the fully synchronized state and the twisted state are stable, a system shows either state depending on initial conditions [14].

This multistability has sparked extensive studies on the basin of attraction of twisted states in the Kuramoto model [12,15,16]. Researchers have particularly focused on determining the conditions under which twisted states remain stable, especially in scenarios with identical Kuramoto oscillators with a strict interaction range [17–19]. For example, it is found that twisted states can be observed in a ring of Kuramoto oscillators when the interaction range is smaller than a critical value, while only a fully synchronized state appears once the interaction range is long enough [20].

One intriguing example for which twisted states may be observed is a large stadium. When audiences sing a national anthem before a baseball game, we can hear people sing in a round, even though the audiences try to synchronize their singing. In this paper, we investigate the condition under which stable twisted states can emerge in such a system. Our specific focus is on Kuramoto oscillators arranged in a circular formation on a two-dimensional (2D) plane. The oscillators have power-law decaying coupling strength and time delay depending on the distance between oscillators, motivated by the case of the stadium.

We uncover that the stability of twisted states is determined by two key factors: the power-law exponent $\alpha$, which regulates the strength of interaction decay, and the speed $v$ of phase information transfer. The exponent $\alpha$ controls the effective interaction range, i.e., the larger $\alpha$ is the shorter the interaction range becomes, and the speed $v$ governs the time delay; i.e., a larger $v$ means a shorter time delay. Without time delay, we find that a critical threshold $\alpha_c$ emerges; the fully synchronized state is the only stable fixed point for $\alpha < \alpha_c$, while twisted states become stable for $\alpha > \alpha_c$. When time delay is introduced, the speed $v$ of information propagation also plays a role. A smaller $v$, indicating a larger time delay, destabilizes the fully synchronized state and stabilizes the twisted states, even for $\alpha < \alpha_c$.

The present paper is structured as follows. In Sec. II, we introduce our model, featuring identical Kuramoto oscillators arranged on the rim of a circle in a 2D plane. In Sec. III, we show that twisted states and a fully synchronized state are

*Corresponding author: beomjun@skku.edu
†Corresponding author: hyejin.park@inha.ac.kr

 

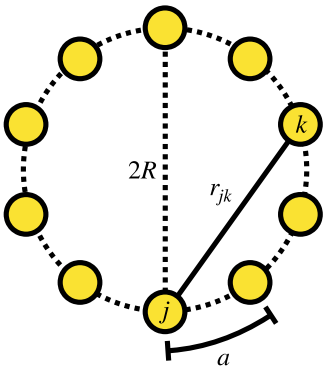


FIG. 1. A schematic diagram of the model [see Eq. (1)]. Equally spaced $N(=10)$ Kuramoto oscillators are on a rim of a planar circle, with the oscillator index $j$ increasing counterclockwise. The distance $a$ between neighboring oscillators along the circumference is assumed to be identical, which plays the role of the lattice constant, and thus the radius of the whole circle is given by $R = Na/2\pi$. As shown, the distance $r_{jk}$ between two oscillators $j$ and $k$ is measured by the two-dimensional Euclidean distance.

fixed points of the model. Then, we present the linear stability analysis with and without the time delay in Sec. IV, providing the main results with an analytic calculation for the transition point $\alpha_c$. Finally, in Sec. V, we conclude with a summary and discussion of our findings.

## II. MODEL

We consider a system of $N$ Kuramoto oscillators [7] on a rim of a planar circle as depicted in Fig. 1. The distance between the nearest-neighboring oscillators along the circumference is fixed to a constant $a$. Then the radius of the circle $R = Na/2\pi$ depends on the system size $N$. With the origin (0,0) at the center of the circle, the $j$th oscillator is located at $(x_j,\ y_j) = [R\cos(2\pi j/N),\ R\sin(2\pi j/N)]$, with $j = 0, 1, \ldots, N-1$.

Assuming power-law decaying interaction coupling and time delay, the phase dynamics of an oscillator $j$ is given by the equations of motion

$$\dot{\theta}_j = \omega + \frac{K}{N}\sum_{k\neq j} r_{jk}^{-\alpha}\sin[\theta_k(t-\tau_{jk}) - \theta_j(t)], \qquad (1)$$

where the overall magnitude of the coupling strength is determined by a constant $K$. Note that we have assumed that all oscillators have identical intrinsic frequencies $\omega_j = \omega$. A coupling strength between oscillators $j$ and $k$ decays in the Euclidean distance $r_{jk} = \sqrt{(x_j - x_k)^2 + (y_j - y_k)^2}$ with the power-law exponent $\alpha$ that controls the heterogeneity of the interaction strength in distance.

The distance-dependent time delay between oscillators $j$ and $k$ is written as $\tau_{jk} = r_{jk}/v$, where $v$ denotes the speed at which the phase information propagates in the system. The interaction heterogeneity in our model is governed by two variables $r_{jk}$ and $\tau_{jk}$ whose effects vanish for $\alpha = 0$ and $v = \infty$, respectively. For the limiting case of $\alpha = 0$, our model becomes completely identical to the original fully connected Kuramoto model.

For further analysis, we make our model equation (1) dimensionless by rescaling the length and the time as $t \to \omega t$, $\tau_{jk} \to \omega\tau_{jk}$, $r_{jk} \to r_{jk}/a$, and $K \to K/(\omega a^\alpha)$, which leads to

$$\dot{\theta}_j = 1 + \frac{K}{N}\sum_{k\neq j} r_{jk}^{-\alpha}\sin[\theta_k(t-\tau_{jk}) - \theta_j(t)]. \qquad (2)$$

When two oscillators $j$ and $k$ are closely located along the circle so that $|j-k|/N \ll 1$, our rescaled distance can be approximated as $r_{jk} \approx |j-k|$ and the interaction strength for the $l$th nearest neighbor ($l = 1, 2, \ldots$) is simply proportional to $l^{-\alpha}$. Consequently, as $\alpha \to \infty$, only the terms at $l = 1$ dominate and the model contains only the nearest-neighbor interactions. Also, when $|j-k|/N \ll 1$, the time delay $\tau_{jk} \approx |j-k|/v$ in the dimensionless form, and thus the time delay for the $l$th nearest-neighbor scales linearly with $l$. Considering both effects on the power-law interaction strength and the spatial time delay, it is probable that our model for $\alpha \to \infty$ behaves as a 1D system with local interaction, for which stable twisted states have been well observed [15,16,20].

For uniformly twisted states, on which the present work mostly puts focus, all oscillators are phase-locked, and the phase difference between each oscillator and its nearest neighbor is constant such that the phase of the $j$th oscillator is written as $\theta_j^{(p)} = 2\pi pj/N + \Omega t$. Here, $\Omega$ represents the phase velocity common to all oscillators, and the integer $p$ is called the winding number and denotes how many times the phases are twisted counterclockwise along the whole system. Note that the value of $p$ can easily distinguish the fully synchronized state ($p = 0$) and the uniformly twisted state ($p \neq 0$).

## III. FIXED POINTS

If twisted states are stable fixed points of the dynamics, oscillators are phase-locked at a certain phase velocity $\Omega$, and we have $\dot{\theta}_j = \Omega$ for all $j$. We use two different approaches depending on the magnitude of the time delay. For a small time delay, our model can be written in an algebraic form, and it is straightforward to prove that the twisted states are stationary solutions. On the contrary, our model cannot be written in an algebraic form when the time delay is relatively large. For this case, we numerically show that twisted states are stationary solutions using a self-consistency equation.

### A. Small time delay

First, we consider the case where the overall time delay in the system is sufficiently small. To write our model in an algebraic form, we drop the constant phase velocity term in Eq. (2). In a frame rotating with an angular velocity $\omega' = 1$ in units of $\omega$, the constant angular velocity term in the right-hand side of Eq. (2) drops, and since $\theta_j(t) \to \theta_j(t) - \omega' t$ with $\omega' = 1$, we obtain

$$\dot{\theta}_j = \frac{K}{N}\sum_{k\neq j} r_{jk}^{-\alpha}\sin[\theta_k(t-\tau_{jk}) - \theta_j(t) - \tau_{jk}]. \qquad (3)$$

We want to show that oscillators in a twisted state have an identical phase velocity. To check that, we apply a uniform twisted solution in Eq. (3) and calculate the phase velocity $\dot{\theta}_j$, which is not an easy task because Eq. (3) contains sine

functions. The problem becomes more tractable when the equation is written in the following form,

$$\dot{\theta}_j = \tfrac{1}{2}(\dot{\tilde{\theta}}_j + (\dot{\tilde{\theta}}_j)^*), \tag{4}$$

where a new variable $\dot{\tilde{\theta}}_j$ is defined as

$$i\dot{\tilde{\theta}}_j \equiv \sum_{k=0}^{N-1} A_{jk} e^{i[\tilde{\theta}_k(t-\tau_{jk})-\tilde{\theta}_j(t)-\tau_{jk}]}, \tag{5}$$

with the interaction strength $A_{jk} = K/(Nr_{jk}^{\alpha})$ with $A_{jj} = 0$. The summation runs for $k = 0$ to $N-1$ as we set the index to start from 0, and the constraint $k \neq j$ is released because $A_{jj} = 0$. Although the phase velocity $\dot{\theta}_j$ in our model is real-valued, we cannot guarantee that the new variable $\dot{\tilde{\theta}}_j$ is also real-valued. Therefore, we allow $\dot{\tilde{\theta}}_j$ to be a complex number. We follow the method presented in Refs. [21–23] to compute $\dot{\theta}_j$ in Eq. (5), with a slight modification since $\gamma$ introduced in Refs. [21–23] is not necessary in our work.

When the time delay is small enough, we can expand $\tilde{\theta}_k(t-\tau_{jk})$ up to the first order of $\tau_{jk}$ as

$$i\dot{\tilde{\theta}}_j = e^{-i\tilde{\theta}_j} \sum_{k=0}^{N-1} A_{jk} e^{i\tilde{\theta}_k} e^{-i\tau_{jk}\dot{\tilde{\theta}}_k} e^{-i\tau_{jk}}. \tag{6}$$

This approximation is valid for $\max(\{\tau_{jk}\}) < 1$, which is equivalent to the condition that $2R/v < 1$ or $v > N/\pi$. However, our approximation can be applied to larger time delays when the effective interaction range becomes smaller. Again, we keep only the terms in Eq. (6) up to the first order of $\tau_{jk}$ and get

$$i\dot{\tilde{\theta}}_j = e^{-i\tilde{\theta}_j} \sum_{k=0}^{N-1} A_{jk}(1 - i\tau_{jk} - i\tau_{jk}\dot{\tilde{\theta}}_k) e^{i\tilde{\theta}_k}. \tag{7}$$

The above equation is written in a matrix form explicitly,

$$\frac{d}{dt}\sum_{k=0}^{N-1} \delta_{jk} e^{i\tilde{\theta}_k} = \sum_{k=0}^{N-1} \left\{ A_{jk} e^{i\tilde{\theta}_k} - iB_{jk} e^{i\tilde{\theta}_k} - B_{jk}\frac{d}{dt} e^{i\tilde{\theta}_k} \right\}, \tag{8}$$

where $B_{jk} = A_{jk}\tau_{jk}$. Note that $A$ and $B$ are real-valued circulant matrices. Collecting the time derivative terms into the left-hand side, we finally obtain the linearized equation

$$\dot{\vec{z}} = (I+B)^{-1}(A - iB)\vec{z}, \tag{9}$$

where $\vec{z} = [\exp(i\tilde{\theta}_0), \exp(i\tilde{\theta}_1), \ldots, \exp(i\tilde{\theta}_{N-1})]^T$. If the time delay is absent ($B = 0$), Eq. (9) is equivalent to

$$\dot{\vec{z}} = A\vec{z}, \tag{10}$$

which gives results similar to those of Ref. [21].

We can calculate the phase velocity of each oscillator using Eq. (9). Let us consider a vector $\vec{\tilde{\theta}} = (\tilde{\theta}_0, \tilde{\theta}_1, \ldots, \tilde{\theta}_{N-1})^T$. The phase velocity vector $\dot{\vec{\tilde{\theta}}}$ can be written explicitly by

$$\dot{\vec{\tilde{\theta}}} = -i\,\mathrm{diag}[\vec{z}]^{-1}\dot{\vec{z}}, \tag{11}$$

where $\mathrm{diag}[\vec{z}]$ is a diagonal matrix whose diagonal elements are elements of $\vec{z}$.

We apply the uniform twisted states solution $\theta_j^{(p)} = 2\pi pj/N + \Omega t$ to Eq. (9) and check that the phase velocities of oscillators are identical using Eq. (11). The method is described in Refs. [17–19]. Let us try $\vec{z} = \vec{z}_p = [\exp(i\theta_0^{(p)}), \ldots, \exp(i\theta_{N-1}^{(p)})]^T$ in Eq. (9) and plug the expression of $\dot{\vec{z}}_p$ into Eq. (11). Since $A$, $B$, and $I$ are circulant matrices, $(I+B)^{-1}A$ and $(I+B)^{-1}B$ are also circulant matrices. Because $\vec{z}_p$ are eigenvectors of circulant matrices, we get

$$i\,\mathrm{diag}[\vec{z}_p]\dot{\vec{\theta}}^{(p)} = \lambda_p[(I+B)^{-1}A]\vec{z}_p \tag{12}$$

$$- i\lambda_p[(I+B)^{-1}B]\vec{z}_p, \tag{13}$$

where $\lambda_p(X)$ is an eigenvalue of the matrix $X$ for the corresponding eigenvector $\vec{z}_p$.

The eigenvalues of $(I+B)^{-1}A$ and $(I+B)^{-1}B$ have only real values because they are circulant matrices. Then the real and imaginary parts of $\dot{\vec{\tilde{\theta}}}$ are given as follows,

$$\mathrm{Re}\,\dot{\vec{\tilde{\theta}}}^{(p)} = -\lambda_p[(I+B)^{-1}B]\mathbf{1} \tag{14}$$

and

$$\mathrm{Im}\,\dot{\vec{\tilde{\theta}}}^{(p)} = -\lambda_p[(I+B)^{-1}A]\mathbf{1}. \tag{15}$$

This result implies that, in the twisted state, our model in Eq. (3) is phase-locked with the following phase velocity:

$$\dot{\vec{\theta}}^{(p)} = \mathrm{Re}\,\dot{\vec{\tilde{\theta}}}^{(p)} = -\lambda_p[(I+B)^{-1}B]\mathbf{1}. \tag{16}$$

In a frame that does not rotate, the oscillators are phase-locked at an angular velocity of

$$\Omega = 1 - \frac{\lambda_p(B)}{1+\lambda_p(B)}, \tag{17}$$

which depends on the winding number $p$. In the absence of time delay ($B = 0$), oscillators are phase-locked at $\Omega = 1$ regardless of $p$. Altogether, the synchronized state and the uniform twisted states are fixed points in a frame rotating with the phase velocity $\Omega$ in Eq. (17) when there is no time delay or the time delay is small. Note that we have not yet investigated the stability of these fixed points; this is pursued in Sec. IV A.

### B. Large time delay

We consider the case where the time delay between oscillators is relatively large. In this case, the method we used earlier to calculate the phase velocity of oscillators directly is not valid. Instead, we demonstrate that uniform twisted states are stationary solutions in our model. When the uniform twisted state solution $\theta_j^{(p)} = 2\pi jp/N + \Omega t$ is applied to Eq. (2), we get the following consistency equation of $\Omega$,

$$\Omega = 1 + \frac{K}{N}\sum_{k\neq j}^{N} r_{jk}^{-\alpha} \sin[2\pi(k-j)p/N - \Omega\tau_{jk}]. \tag{18}$$

We numerically confirm that the consistency equation has indeed one solution for each parameter set considered in this study. Therefore, the uniform twisted states are fixed points in a rotating frame that has the phase velocity $\Omega$. In fact, the

left-hand side of Eq. (18) is a linear function of $\Omega$ while the right-hand side is a linear combination of a constant and sine functions with the period of $2\pi/\tau_{ij}$, resulting in oscillations around the constant term. Hence, there is always at least one solution.

Altogether, we conclude that the synchronized state and the uniform twisted states are fixed points in our model. Although there may be other fixed points besides the uniform twisted states, identifying such points is beyond the scope of this paper. Therefore, we focus only on the fully synchronized state and the uniform twisted states, and their stability is investigated in Sec. IV B.

## IV. LINEAR STABILITY ANALYSIS

In the previous section, we showed that the synchronized state and the uniform twisted states are fixed points in our model. Now we consider the linear stability of these states in the model using the Jacobian matrix of Eq. (2).

By assuming that the oscillators are phase-locked at the phase velocity $\Omega$ in Eq. (2), we get

$$\dot{\theta}_j = 1 + \frac{K}{N}\sum_{k\neq j}^{N} r_{jk}^{-\alpha}\sin\left(\theta_k - \theta_j - \Omega\tau_{jk}\right). \tag{19}$$

The Jacobian matrix element $J_{ab} = \partial f_a/\partial\theta_b$ of the above equation with $f_j(\{\theta_k\}) = \dot{\theta}_j$ at the twisted states $\theta_j^{(p)} = 2\pi pj/N + \Omega t$ is

$$J_{ab}^{(p)} = \begin{cases} A_{ab}\cos\left(\theta_b^{(p)} - \theta_a^{(p)} - \Omega\tau_{ab}\right) & (a\neq b), \\ -\sum_k A_{ak}\cos\left(\theta_k^{(p)} - \theta_a^{(p)} - \Omega\tau_{ak}\right) & (a = b). \end{cases} \tag{20}$$

The Jacobian matrix in Eq. (20) is circulant when (i) time delay is absent ($\tau_{ab} = 0$) or (ii) oscillators are fully synchronized even with time delay ($p = 0$).

### A. Stability of twisted states without time delay

We consider the first case where time delay is absent. When there is no time delay ($\tau_{ab} = 0$), the Jacobian matrix becomes

$$J_{ab}^{(p)} = \begin{cases} A_{ab}\cos\left(\theta_b^{(p)} - \theta_a^{(p)}\right) & (a\neq b), \\ -\sum_{k=0}^{N-1} A_{ak}\cos\left(\theta_k^{(p)} - \theta_a^{(p)}\right) & (a = b), \end{cases} \tag{21}$$

which has the same form as the Jacobian matrix in Ref. [18]. Because $J_{ab}^{(p)}$ only depends on the value of $|a-b|$, the Jacobian matrix in Eq. (21) is a circulant matrix. Therefore, eigenvalues of the Jacobian matrix are given in the following closed form [18],

$$\begin{aligned}\Lambda_r(J^{(p)}) &= \sum_{s=1}^{N-1} A_s\cos(pt_s)[\cos(rt_s) - 1] \\ &\propto \sum_{s=1}^{N-1}\frac{\cos(rt_s) - 1}{[1-\cos(t_s)]^{\alpha/2}}\cos(pt_s),\end{aligned} \tag{22}$$

where $t_s = 2\pi s/N$, $A_s = A_{s'(s'+s)}$, and $\Lambda_r(X)$ is the $r$th eigenvalue of a matrix $X$. As the term for $s = 0$ has a null contribution, the summation runs from $s = 1$.

Figure 2 shows the linear stability of the synchronized state ($p = 0$) and the twisted states ($p \neq 0$) without time delay for different values of $\alpha$ using parameters $N = 300$ and $K = 1$.

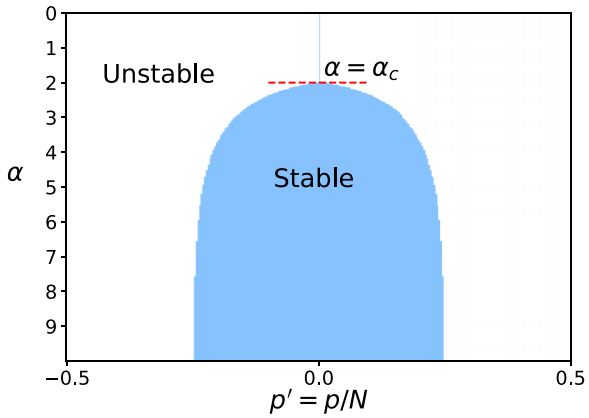


FIG. 2. The stability diagram of the model in Eq. (2) with parameters $N = 300$ and $K = 1$. The blue and white regions correspond to the linearly stable and unstable regions for given values of $\alpha$ and $p' = p/N$. The fully synchronized state ($p = 0$) is linearly stable for all values of $\alpha$ (note that there is a thin vertical line structure at $p' = 0$) while twisted states ($p \neq 0$) start to become linearly stable at the critical point $\alpha_c \approx 2$. More twisted states become stable as $\alpha$ increases.

We determine the linear stability by numerically evaluating the signs of the summation for all possible $r$ in Eq. (22). We use the normalized winding number $p' = p/N$, and the stability diagram converges as the population size $N$ increases. The diagram is symmetric for the vertical line $p' = 0$ because the model does not favor a particular direction of winding.

As $\alpha$ increases from 0 to 10, the stability of twisted states changes from unstable to stable. For small values of $\alpha$, the synchronized state marked by the zero winding number $p = 0$ is the only stable state. Other twisted states become stable as $\alpha$ increases over a critical value of $\alpha_c \approx 2$. We provide quantitative analysis for $\alpha_c$ below, after interpreting the results in Fig. 2. The fully synchronized state is linearly stable for all values of $\alpha$ considered in Fig. 2.

The main mechanism explaining the change in linear stability of twisted states is that the exponent $\alpha$ controls the effective interaction structure from the global coupling ($\alpha = 0$) to the nearest-neighbor coupling ($\alpha \to \infty$). The effective interaction range decreases as $\alpha$ increases from 0, resulting in stable twisted states. This result is consistent with the previous study [20] where the identical Kuramoto oscillators are considered on a one-dimensional chain with a strict interaction range $L$. In that system, stable twisted states appear as the interaction range becomes shorter while the system converges to the synchronized state when $L$ is larger than the critical interaction range $L_c$ [20].

In Fig. 2, the rescaled winding number $p'$ of stable twisted states spans the range from $-1/4$ to $1/4$, although $p'$ can have values from $-1/2$ to $1/2$ by its definition. The restriction of $p'$ can be understood in a heuristic manner. In the limit $\alpha \to \infty$, two dominant terms, $s = 1$ and $s = N-1$ in Eq. (22), determine the stability of given twisted states. Then, the stability is determined by the sign of

$$-2\frac{1-\cos(rt_1)}{[1-\cos(t_1)]^{\alpha/2}}\cos(pt_1). \tag{23}$$

Note that $1-\cos(t_1)$ and $1-\cos(rt_1)$ are always greater than or equal to 0. Therefore, $\cos(pt_1)$ solely determines the sign of the eigenvalue. For obtaining negative eigenvalues, $pt_1$ should be in the range $(-\pi/2, \pi/2)$, and thus $p' \in (-1/4, 1/4)$.

In Fig. 2, a critical value of $\alpha$ marks the appearance of stable twisted states. We analytically derive the equation for $\alpha_c$ using Eq. (22) and numerically estimate the solution. In the vicinity of $\alpha_c$ ($\alpha \leqslant 2$), we have numerically checked that $\Lambda_p(J^{(p)})$ is the largest eigenvalue among $\Lambda_r(J^{(p)})$ (data not shown here). Therefore, we can determine the linear stability of the twisted state with $p$ by investigating the sign of $\Lambda_p(J^{(p)})$, which changes from positive to negative when the stability changes. Since $p = \pm 1$ states first become linearly stable as $\alpha$ increases, we assume that $\Lambda_1(J^{(1)})$ becomes 0 at the transition point $\alpha_c$ and we use this condition to find $\alpha_c$.

Setting $p = 1$ and $r = 1$ in Eq. (22), we obtain

$$\Lambda_1(J^{(1)}) \propto -\sum_{s=1}^{N-1} \sin^{2-\alpha}\left(\frac{t_s}{2}\right)\cos(t_s) \tag{24}$$

$$\propto -\sum_{s=1}^{N-1} \sin^{2-\alpha}\left(\frac{t_s}{2}\right) + 2\sum_{s=1}^{N-1} \sin^{4-\alpha}\left(\frac{t_s}{2}\right). \tag{25}$$

For a large $N$, we take the continuum limit of Eq. (25). Then the condition $\Lambda_1(J_1) = 0$ at the transition point $\alpha_c$ is written as

$$\int_{\delta}^{\pi-\delta} d\theta \sin^{2-\alpha_c}\theta = 2\int_{\delta}^{\pi-\delta} d\theta \sin^{4-\alpha_c}\theta, \tag{26}$$

where $\delta = \pi/N$. The above equation is further simplified to

$$\frac{(\alpha_c-2)}{2}\,{}_2F_1\left[\frac{1}{2}, \frac{\alpha_c-1}{2}, \frac{3}{2}, \cos^2\delta\right] = \sin^{3-\alpha_c}\delta, \tag{27}$$

where ${}_2F_1$ is a hypergeometric function.

In a large system, $\delta = \pi/N$ is small enough that we can use the small-angle approximation, $\sin\delta \sim \delta$ and $\cos\delta \sim 1$. Then we have

$$\frac{(\alpha_c-2)}{2}\,{}_2F_1\left[\frac{1}{2}, \frac{\alpha_c-1}{2}, \frac{3}{2}, 1\right] = \delta^{3-\alpha_c}. \tag{28}$$

Finally, we get the equation for the transition point:

$$\frac{\sqrt{\pi}(\alpha_c-2)}{4}\frac{\Gamma[(3-\alpha_c)/2]}{\Gamma[(4-\alpha_c)/2]} = \delta^{3-\alpha_c}. \tag{29}$$

We note that the transition point $\alpha_c$ only depends on the size of the system $N$. The numerical solution $\alpha_c$ of Eq. (29) is presented in Fig. 3 as a function of the number of oscillators $N$. As the size of the system increases, the transition point $\alpha_c$ approaches an asymptotic line drawn at $\alpha_c = 2$.

### B. Effect of time delay

Now we consider the time delay ($\tau_{ab} = r_{ab}/v \neq 0$). The Jacobian matrix in Eq. (20) is circulant only for the synchronized state ($p = 0$). Thus, the exact eigenvalue of the Jacobian can be computed only for the synchronized state. For twisted states ($p \neq 0$), we numerically evaluate the eigenvalues of the Jacobian and determine their stability.

Figure 4(a) shows the linear stability of the synchronized state for different values of $\alpha$ and $v$. The stability is determined by the following eigenvalues [18]:

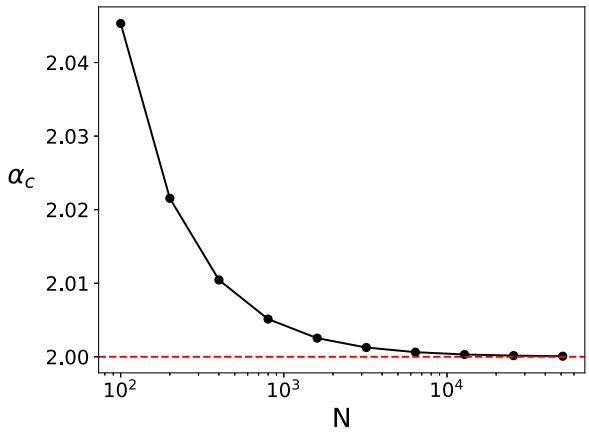


FIG. 3. The transition point $\alpha_c$ is estimated by the solution of Eq. (29) at the given number of oscillators $N$. The red horizontal line shows the asymptotic value, 2. The transition point $\alpha_c$ approaches 2 as the size of the system increases.

$$\Lambda_r'(J^{(0)}) \propto \sum_{s=1}^{N-1} \frac{\cos(rt_s)-1}{[1-\cos(t_s)]^{\alpha/2}}\cos(\Omega\tau_s), \tag{30}$$

which are the eigenvalues of the Jacobian in Eq. (20) for $\tau_{ab} = r_{ab}/v \neq 0$ and $p = 0$. The phase-locked velocity $\Omega$ is calculated by solving the consistency equation in Eq. (18). We can easily see that there is a certain area of $(\alpha, v)$ in which the fully synchronized state is unstable, unlike the result in Fig. 2 where the fully synchronized state is stable for all values of $\alpha$ considered.

As expected, when the propagation speed of the phase information $v$ is large enough, the time delay between oscillators is negligible and the fully synchronized state is stable for all values of $\alpha$. We note that $1-\cos(t_s)$ is positive for $s = 1, \ldots, N-1$ in Eq. (30), and thus we conclude a strict condition for the synchronized state to be stable is given by $\cos(\Omega\tau_s) > 0$. This condition is similar to the condition $\cos(\Omega\tau) > 0$ in Ref. [24] for the mean-field Kuramoto oscillators with identical time delay $\tau$. For small time delay (high-$v$ regime), the condition $\cos(\Omega\tau_s) > 0$ is satisfied ($\Omega\tau_s < \pi/2$). As $v$ decreases, however, time delay acts as a disturbance to the system and the synchronized state becomes unstable.

On the other hand, the power-law exponent $\alpha$ can also influence the time delay effect since $\alpha$ controls the effective interaction range between oscillators. As $\alpha$ is increased, the large time delay between distant oscillators becomes meaningless because effective interaction becomes short-ranged. Therefore, the synchronized state is again stable in the large-$\alpha$ regime with a large time delay.

Besides the synchronized state, the stability of twisted states is also affected by time delay according to $v$. A stability diagram of twisted states is shown in Fig. 4(b). The stability is determined by eigenvalues of the Jacobian in Eq. (20), which are numerically evaluated. We observe that the fully synchronized state ($p = 0$) in Fig. 4(b) becomes unstable for small $\alpha$ while $p = \pm 1$ states become stable. This result is quite different from the result in Fig. 2, where the only stable fixed point is the synchronized state for $\alpha < \alpha_c$.

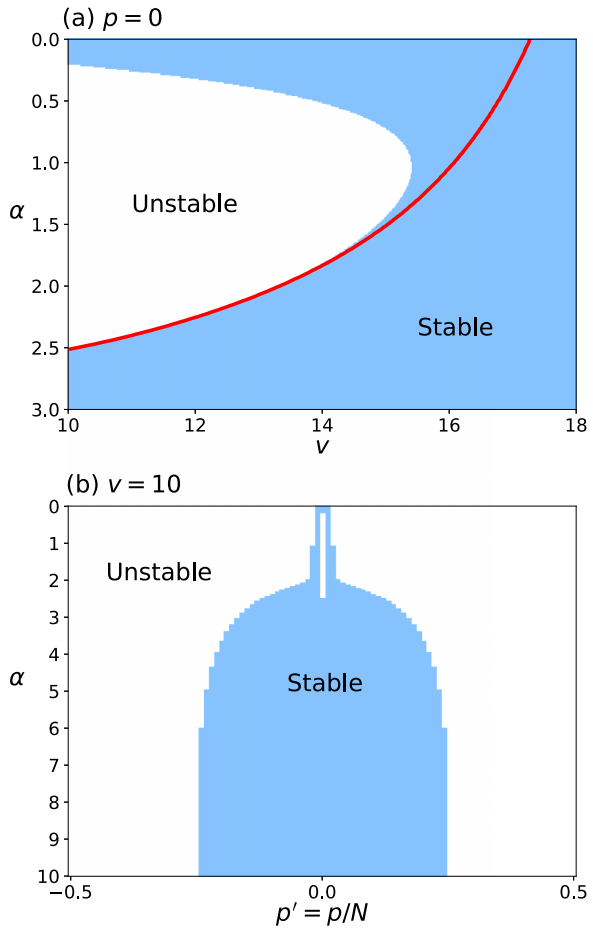


FIG. 4. Stability diagrams of the model in Eq. (2) for $N = 100$ and $K = 1$. (a) Stability of the synchronized state ($p = 0$) in the plane of $\alpha$ and $v$. The red solid line marks the boundary between the stable and unstable regions estimated with $\Omega$ calculated by Eq. (17), which assumed small time delay. The line well matches the actual boundary for relatively large $\alpha$. (b) Stability of the synchronized ($p = 0$) and twisted ($p \neq 0$) states at $v = 10$. At low $v$, time delay makes the synchronized state unstable when the system moves away from the mean-field regime. However, the synchronized state regains its stability with large $\alpha$. That is because the effect of large time delay with faraway oscillators becomes less important as the effective interaction range shrinks.

When the time delay with oscillator $\tau_s$ is small, we can expand Eq. (30) up to the second order of $\Omega\tau_s$. Then $\Lambda_r'(J^{(0)})$ is represented by a linear combination of $\Lambda_r(J^{(0)})$ and $\Lambda_r(J^{(1)})$,

$$\Lambda_r'(J^{0)}) = \Lambda_r(J^{(0)}) - \eta^2\{\Lambda_r(J^{(0)}) + \Lambda_r(J^{(1)})\}. \tag{31}$$

The parameter $\eta$ is defined as

$$\eta = \left(\frac{1}{v'}\right)\left(\frac{2\pi}{\Omega}\right)^{-1}, \tag{32}$$

which is a ratio between two timescales; $2\pi/\Omega$ is a period of phase-locked oscillators, and $1/v'$ is a time delay between two consecutive oscillators for the rescaled velocity $v' = v/N$. In the limit $v' \to \infty$, $\eta$ goes to 0, and we recover the eigenvalues without time delay: $\Lambda_r'(J^{(0)}) = \Lambda_r(J^{0)})$.

## V. SUMMARY AND DISCUSSION

In this paper, we investigated the linear stability of the fully synchronized state and the twisted states for identical Kuramoto oscillators on a planar circle. In our model, all oscillators are fully connected, and the strength of their interactions decays in a power-law form with the Euclidean distance in two-dimensional space. We explored two distinct scenarios: one where there is no time delay and another where distance-related time delays are introduced.

In the absence of time delay, the exponent $\alpha$ plays a crucial role in determining the stability of states by altering the effective interaction range. For $\alpha < \alpha_c$, the synchronized state is the only stable fixed point. Twisted states become stable as $\alpha$ exceeds the transition threshold $\alpha_c$. We derived an equation for $\alpha_c$ and found that the solution depends on the size of the system $N$, converging towards 2 as $N \to \infty$.

On the other hand, the time delay between oscillators also affects the stability. The speed at which phase information propagates, denoted as $v$, is critical to understanding the stability. We found that, when the speed $v$ is small, the time delays between oscillators are not negligible, and the stability changes. For instance, while the synchronized state remains stable across all values of $\alpha$ in the absence of time delay, it becomes unstable within certain regions of $\alpha$ in the low-$v$ regime characterized by slow information propagation. In this case, stable twisted states can appear even for $\alpha < \alpha_c$. It gives a clue to the reason why people sing in a round in a large stadium. Even when $\alpha = 2 \lesssim \alpha_c$, which we believe corresponds to the realistic case of sound propagation, the synchronized state might become unstable in such a system due to the time delay.

Our study raises intriguing questions about the transition point $\alpha_c$. While we were able to derive the equation for $\alpha_c$, the fundamental reasons behind why $\alpha_c \approx 2$ remain unclear. Additionally, our focus was primarily put on the first appearance of stable twisted states marked by $\alpha_c$. However, each distinct twisted state has its own transition point $\alpha_c^{(p)}$, as illustrated in Fig. 2. Exploring and calculating these transition points for $p$-twisted states $\alpha_c^{(p)}$ can be an interesting avenue for future research.

Finally, we could also think about the basin of attraction. The linear stability analysis can only detect whether the system will stay in or escape from a given state. However, it could also be important to know the basin of attraction for each stable state. To estimate the size of basins, one could run a series of simulations starting from the incoherent state and calculate the probability density for the winding number $p$ in the final states as in Refs. [12,20]. This approach would provide valuable insights into the dynamics of the system beyond simple stability considerations.

## ACKNOWLEDGMENTS

This research was supported by grants from the National Research Foundation of Korea (NRF) funded by the Korea government (MSIT), Grants No. 2019R1A2C2089463 (H.S.L. and B.J.K.) and No. RS-2023-00214071 (H.J.P.). This work was supported by a research grant from Inha University as well (H.J.P.).

[1] Z. Néda, E. Ravasz, Y. Brechet, T. Vicsek, and A.-L. Barabási, Nature (London) **403**, 849 (2000).
[2] Z. Néda, E. Ravasz, T. Vicsek, Y. Brechet, and A.-L. Barabási, Phys. Rev. E **61**, 6987 (2000).
[3] Z. Néda, A. Nikitin, and T. Vicsek, Phys. A (Amsterdam, Neth.) **321**, 238 (2003).
[4] D. C. Michaels, E. P. Matyas, and J. Jalife, Circ. Res. **61**, 704 (1987).
[5] B. Eckhardt, E. Ott, S. H. Strogatz, D. M. Abrams, and A. McRobie, Phys. Rev. E **75**, 021110 (2007).
[6] M. M. Abdulrehem and E. Ott, Chaos **19**, 013129 (2009).
[7] J. A. Acebrón, L. L. Bonilla, C. J. P. Vicente, F. Ritort, and R. Spigler, Rev. Mod. Phys. **77**, 137 (2005).
[8] F. A. Rodrigues, T. K. D. Peron, P. Ji, and J. Kurths, Phys. Rep. **610**, 1 (2016).
[9] J. Gómez-Gardenes, S. Gómez, A. Arenas, and Y. Moreno, Phys. Rev. Lett. **106**, 128701 (2011).
[10] B. C. Coutinho, A. V. Goltsev, S. N. Dorogovtsev, and J. F. F. Mendes, Phys. Rev. E **87**, 032106 (2013).
[11] H. Hong, M.-Y. Choi, and B. J. Kim, Phys. Rev. E **65**, 026139 (2002).
[12] D. A. Wiley, S. H. Strogatz, and M. Girvan, Chaos **16**, 015103 (2006).
[13] M. Goebel, M. S. Mizuhara, and S. Stepanoff, Chaos **31**, 103106 (2021).
[14] T. Girnyk, M. Hasler, and Y. Maistrenko, Chaos **22**, 013114 (2012).
[15] K. Dénes, B. Sándor, and Z. Néda, Commun. Nonlinear Sci. Numer. Simul. **78**, 104868 (2019).
[16] K. Dénes, B. Sándor, and Z. Néda, Commun. Nonlinear Sci. Numer. Simul. **93**, 105505 (2021).
[17] R. Yoneda, T. Tatsukawa, and J.-n. Teramae, Chaos **31**, 063124 (2021).
[18] A. Townsend, M. Stillman, and S. H. Strogatz, Chaos **30**, 083142 (2020).
[19] M. Kassabov, S. H. Strogatz, and A. Townsend, Chaos **31**, 073135 (2021).
[20] H. Hong and B. J. Kim, J. Korean Phys. Soc. **64**, 954 (2014).
[21] L. Muller, J. Mináč, and T. T. Nguyen, Phys. Rev. E **104**, L022201 (2021).
[22] R. C. Budzinski, T. T. Nguyen, J. Đoàn, J. Mináč, T. J. Sejnowski, and L. E. Muller, Chaos **32**, 031104 (2022).
[23] R. C. Budzinski, T. T. Nguyen, G. B. Benigno, J. Đoàn, J. Mináč, T. J. Sejnowski, and L. E. Muller, Phys. Rev. Res. **5**, 013159 (2023).
[24] M. K. Stephen Yeung and S. H. Strogatz, Phys. Rev. Lett. **82**, 648 (1999).